

Mass-loss histories of Type II_n supernova progenitors within decades before their explosion

Takashi J. Moriya^{1,2,3*}, Keiichi Maeda^{4,2}, Francesco Taddia⁵, Jesper Sollerman⁵, Sergei I. Blinnikov^{6,7,2}, and Elena I. Sorokina⁸

¹ Argelander Institute for Astronomy, University of Bonn, Auf dem Hügel 71, D-53121 Bonn, Germany

² Kavli Institute for the Physics and Mathematics of the Universe (WPI), Todai Institutes for Advanced Study, University of Tokyo, 5-1-5 Kashiwanoha, Kashiwa, Chiba 277-8583, Japan

³ Research Center for the Early Universe, Graduate School of Science, University of Tokyo, 7-3-1 Hongo, Bunkyo, Tokyo, Japan

⁴ Department of Astronomy, Kyoto University, Kitashirakawa-Oiwake, Sakyo, Kyoto 606-8502, Japan

⁵ The Oskar Klein Centre, Department of Astronomy, Stockholm University, AlbaNova, 10691 Stockholm, Sweden

⁶ Institute for Theoretical and Experimental Physics, Bolshaya Cheremushkinskaya 25, 117218 Moscow, Russia

⁷ Novosibirsk State University, Novosibirsk 630090, Russia

⁸ Sternberg Astronomical Institute, M.V.Lomonosov Moscow State University, Universitetski pr. 13, 119992 Moscow, Russia

Accepted 2014 January 17. Received 2014 January 17; in original form 2013 December 18

ABSTRACT

We present results of a systematic study of the mass-loss properties of Type II_n supernova progenitors within decades before their explosion. We apply an analytic light curve model to 11 Type II_n supernova bolometric light curves to derive the circumstellar medium properties. We reconstruct the mass-loss histories based on the estimated circumstellar medium properties. The estimated mass-loss rates are mostly higher than $10^{-3} M_{\odot} \text{ yr}^{-1}$ and they are consistent with those obtained by other methods. The mass-loss rates are often found to be constantly high within decades before their explosion. This indicates that there exists some mechanism to sustain the high mass-loss rates of Type II_n supernova progenitors for at least decades before their explosion. Thus, the shorter eruptive mass loss events observed in some Type II_n supernova progenitors are not always responsible for creating their dense circumstellar media. In addition, we find that Type II_n supernova progenitors may tend to increase their mass-loss rates as they approach to the time of their explosion. We also show a detailed comparison between our analytic prediction and numerical results.

Key words: circumstellar matter — stars: mass-loss — supernovae: general

1 INTRODUCTION

Type II_n supernovae (SNe II_n) which were first named by Schlegel (1990) are a subclass of SNe II. They show narrow emission components in their spectra which are presumed to be related to the existence of dense circumstellar media (CSM) near the SN progenitors (e.g., Chugai & Danziger 1994; Fransson et al. 2002). The existence of the dense CSM indicates that the SN II_n progenitors have high mass-loss rates shortly before the explosion. Indeed, some SNe II_n are related to luminous blue variables (LBVs) which are at an evolutionary stage of very massive stars (Humphreys & Davidson 1994). For instance, the progenitors of SNe II_n 2005gl, 2009ip, and 1961V are found to be consistent with LBVs (e.g., Gal-Yam & Leonard 2009; Mauerhan et al. 2013b; Smith et al. 2011). However, LBVs

have not been considered to be SN progenitors in the theoretical stellar evolution perspective (e.g., Langer 2012), although theoretical investigation of a possible LBV-like SN progenitor is starting to appear (Groh, Meynet, & Ekström 2013). In addition, not all SNe II_n are related to very massive stars like LBVs, but a large fraction of them may come from less massive stars (e.g., Prieto et al. 2008; Anderson et al. 2012).

Estimating mass-loss histories of SN II_n progenitors is essential for understanding their progenitors and mass-loss mechanisms. Mass-loss rates of SN II_n progenitors have been estimated in many ways. The line strength of H α in SNe II_n is an observational property often used to estimate the CSM density and thus the mass-loss rate (e.g., Taddia et al. 2013, T13 hereafter; Stritzinger et al. 2012; Kiewe et al. 2012). The dust emission observed in near- and mid-infrared has also been used (Maeda et al. 2013; Fox et al. 2011, 2013 and references therein). X-ray observations are also widely used

* moriyatk@astro.uni-bonn.de

to estimate the CSM properties (e.g., Dwarkadas & Gruszko 2012; Chandra et al. 2012a,b; Katsuda et al. 2014). These observations commonly suggest that the mass-loss rates of SN IIn progenitors are typically higher than $10^{-3} M_{\odot} \text{ yr}^{-1}$, which is much higher than those estimated for other core-collapse SN progenitors ($\sim 10^{-5} M_{\odot} \text{ yr}^{-1}$ or less, e.g., Chevalier, Fransson, & Nymark 2006; Chevalier & Fransson 2006).

In a previous paper of ours (Moriya et al. 2013c, M13 hereafter), we developed an analytic bolometric light-curve (LC) model for SNe IIn which can be used to estimate the CSM properties. We have applied our analytic model to the bolometric LCs reported by Stritzinger et al. (2012) (SNe 2005ip and 2006jd) and Zhang et al. (2012) (SN 2010jl) in M13. In this paper, we additionally apply our bolometric LC model to those reported by T13, Fassia et al. (2000), Roming et al. (2012), and Fraser et al. (2013a). In total, we estimate the mass-loss histories of 11 SN IIn progenitors and, although the number is still small, we try to see if there are general properties in the mass loss of SN IIn progenitors.

This paper is organized as follows. In Section 2, we shortly summarize our analytic bolometric LC model presented in M13. We apply the LC model to the bolometric LCs in Section 3. We summarize the results in Section 4 and see if there exist general trends in the mass loss properties of SN IIn progenitors shortly before their explosions. We present our conclusions in Section 5. In Appendix A, we present a detailed comparison between our analytic model and numerical results to demonstrate the reliability of our analytic model.

2 BOLOMETRIC LIGHT CURVE MODEL

We briefly summarize the M13 analytic bolometric LC model for SNe whose major power source is the interaction between SN ejecta and its CSM. More detailed information on the model is presented in M13.

The analytic model assumes that the homologously-expanding SN ejecta has two components in the density structure, $\rho_{\text{ej}} \propto r^{-\delta}$ inside and $\rho_{\text{ej}} \propto r^{-n}$ outside, where r is a radius. The parameter n is known to be mostly determined by the compactness of the progenitor from numerical simulations (e.g., Matzner & McKee 1999). For example, explosions of red supergiants end up with $n \simeq 12$ while those of Wolf-Rayet stars lead to $n \simeq 10$. The CSM is assumed to have a single power-law density structure [$\rho_{\text{csm}}(r) = Dr^{-s}$].

We assume that the shocked SN ejecta and CSM form a thin shell because of the efficient radiative cooling so that the shocked region can be expressed with a single radius $r_{\text{sh}}(t)$, where t is the time since the explosion. Then, the evolution of the shell radius can be estimated through the conservation of momentum, i.e.

$$M_{\text{sh}} \frac{dv_{\text{sh}}}{dt} = 4\pi r_{\text{sh}}^2 [\rho_{\text{ej}} (v_{\text{ej}} - v_{\text{sh}})^2 - \rho_{\text{csm}} (v_{\text{sh}} - v_{\text{csm}})^2], \quad (1)$$

where M_{sh} is the total mass of the shocked SN ejecta and CSM, v_{sh} is the velocity of the shell, v_{ej} is the velocity of the SN ejecta at r_{sh} , and v_{csm} is the CSM velocity. The concrete form of Equation (1) differs depending on the SN density structure entering the shell. At first, the outer SN ejecta with $\rho_{\text{ej}} \propto r^{-n}$ enters the shell. After a certain time t_t when the

region in the SN ejecta with $\rho_{\text{ej}} \propto r^{-n}$ is completely swept up, the density structure entering the SN ejecta becomes $\rho_{\text{ej}} \propto r^{-\delta}$.

Assuming that we get a solution for Equation (1), we are able to write down the kinetic energy dE_{kin} entering the shell,

$$dE_{\text{kin}} = 4\pi r_{\text{sh}}^2 \frac{1}{2} \rho_{\text{csm}} v_{\text{sh}}^2 dr_{\text{sh}}. \quad (2)$$

If a fraction ϵ of the kinetic energy is transferred to radiation energy, the SN bolometric luminosity L can be expressed as

$$L = \epsilon \frac{dE_{\text{kin}}}{dt} = 2\pi\epsilon\rho_{\text{csm}}r_{\text{sh}}^2v_{\text{sh}}^3. \quad (3)$$

In this paper, we assume $\epsilon = 0.1$ if necessary as we assume in M13.

It turns out that the bolometric luminosity before $t = t_t$ has a simple power-law form

$$L = L_1 t^\alpha, \quad (4)$$

where L_1 is a constant and

$$\alpha = \frac{6s - 15 + 2n - ns}{n - s}. \quad (5)$$

If we can obtain α by fitting an observed SN bolometric LC before t_t , we can constrain the CSM density slope s just from the bolometric LC by assuming n . If there are spectral observations from which we can infer the shell velocity evolution, we can estimate D in $\rho_{\text{csm}} = Dr^{-s}$ and we can get information on the CSM density structure. Even if there is no velocity information, we can still estimate D by assuming the SN ejecta mass M_{ej} and energy E_{ej} .

After $t = t_t$, there is no general analytic solution to Equation (1) and we do not have a simple expression for L . However, we can solve an asymptotic form of Equation (1) numerically which is applicable at $t \gg t_t$. Then, we can use Equation (3) to estimate the bolometric luminosity.

Once we succeed in estimating the CSM density structure $\rho_{\text{csm}} = Dr^{-s}$, we can estimate the mass-loss rate evolution of the SN progenitor by assuming a constant CSM velocity v_{csm} . This is simply because the CSM at r is ejected at the time $t' = r/v_{\text{csm}}$ before the explosion under this assumption. Then, the mass-loss history $\dot{M}(t')$ is

$$\dot{M}(t') = 4\pi r^2 \rho_{\text{csm}} v_{\text{csm}} = 4\pi D v_{\text{csm}}^{3-s} t'^{2-s}, \quad (6)$$

where t' is the time before the explosion.

3 REVEALING MASS-LOSS HISTORY

We apply the bolometric LC model presented in M13 and summarized in the previous section to the observed SN IIn bolometric LCs in this section. The bolometric LCs of T13, Fassia et al. (2000), and Fraser et al. (2013a) are constructed based on the photometric observations covering from near-ultraviolet to near-infrared. The bolometric LC of SN 2010jl constructed by Zhang et al. (2012) is based only on their optical photometric observations. The bolometric LC of SN 2011ht is based on near-ultraviolet to optical observations (Roming et al. 2012, see also Pritchard et al. 2013).

3.1 SN 2005ip

SN 2005ip has already been modeled in M13. The result of the LC fitting including the statistical error is

$$L = (1.44 \pm 0.08) \times 10^{43} \left(\frac{t}{1 \text{ day}} \right)^{-0.536 \pm 0.013} \text{ erg s}^{-1}. \quad (7)$$

As shown in M13, $\alpha = -0.536 \pm 0.013$ corresponds to $s = 2.28 \pm 0.03$ ($n = 10$) or $s = 2.36 \pm 0.02$ ($n = 12$). Assuming $s = 2.28$, the CSM density structure becomes

$$\rho_{\text{CSM}}(r) = 8.4 \times 10^{-16} \left(\frac{r}{10^{15} \text{ cm}} \right)^{-2.28} \text{ g cm}^{-3}. \quad (8)$$

The corresponding mass-loss history is

$$\dot{M}(t') = 2.3 \times 10^{-3} \left(\frac{v_{\text{CSM}}}{100 \text{ km s}^{-1}} \right)^{0.72} \left(\frac{t'}{1 \text{ year}} \right)^{-0.28} M_{\odot} \text{ yr}^{-1}, \quad (9)$$

where t' is the time before the explosion. The mass-loss rate does not differ much whether we use $n = 10$ or $n = 12$.

3.2 SN 2005kj

The bolometric LC of SN 2005kj declines so rapidly that it is difficult to fit it by the M13 LC model. However, we find that the ‘shell-shocked diffusion’ model (Smith & McCray 2007; Arnett 1980, but see also Moriya et al. 2013a) is consistent with the LC after the peak. The possibility to apply the diffusion model to SNe IIn which cannot be explained by the M13 model is further discussed in M13. The diffusion model is applicable to the declining phase after the shock goes through a dense CSM. The LC evolution is expressed as

$$L = L_0 \exp \left[-\frac{t - t_p}{\tau_{\text{diff}}} \left(1 + \frac{t - t_p}{2\tau_{\text{exp}}} \right) \right], \quad (10)$$

where t_p is the time of the maximum luminosity, τ_{diff} is the characteristic diffusion timescale in the shocked dense CSM, and τ_{exp} is the expansion timescale of the shocked dense CSM.

Fig. 1 shows the result of the fitting to Equation (10) after the LC peak. As the observed LC does not have a clear peak and the epoch of the explosion is not well-determined, we fit the LC assuming several possible t_p . However, we found that the result of the fitting is not very sensitive to the assumed t_p . In Fig. 1, we show the LC obtained by assuming that the first observed LC point is the LC peak ($t_p = 11.8$ days since the explosion, T13). We then obtain $\tau_{\text{diff}} = 175 \pm 9$ days, $\tau_{\text{exp}} = 57 \pm 5$ days, and $L_0 = (5.95 \pm 0.05) \times 10^{42} \text{ erg s}^{-1}$. Here, the errors are the statistical errors. Assuming $t_p = 5$ days, we obtain $\tau_{\text{diff}} = 199 \pm 13$ days, $\tau_{\text{exp}} = 50 \pm 6$ days, and $L_0 = (6.17 \pm 0.06) \times 10^{42} \text{ erg s}^{-1}$. In the most extreme case ($t_p = 0$ days), we instead find $\tau_{\text{diff}} = 221 \pm 17$ days, $\tau_{\text{exp}} = 45 \pm 5$ days, and $L_0 = (6.32 \pm 0.07) \times 10^{42} \text{ erg s}^{-1}$.

We can roughly estimate the mass-loss rate of the progenitor from the diffusion timescale. The diffusion timescale can be approximated as

$$\tau_{\text{diff}} \sim \frac{\kappa \bar{\rho} R^2}{c}, \quad (11)$$

where κ is the opacity of the dense CSM, $\bar{\rho}$ is the average density of the CSM, R is the radius of the CSM, and c is the speed of light. Then, the CSM mass M_{CSM} is roughly

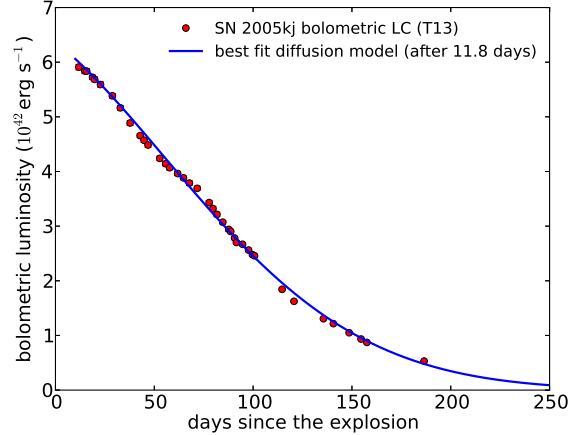


Figure 1. Bolometric LC of SN 2005kj from T13 and a model fit to it based on the diffusion model. The diffusion model in the figure is obtained assuming that the LC peak is 10 days after the explosion.

$$M_{\text{CSM}} = \frac{4}{3} \pi \bar{\rho} R^3 \sim \frac{4\pi c \tau_{\text{diff}} R}{3\kappa}. \quad (12)$$

If M_{CSM} is ejected in a time Δt , the mass-loss rate can be approximated as $\dot{M} \sim M_{\text{CSM}}/\Delta t$. As $\Delta t = R/v_{\text{CSM}}$, we get

$$\dot{M} \sim \frac{4\pi c \tau_{\text{diff}} v_{\text{CSM}}}{3\kappa}. \quad (13)$$

Using $\tau_{\text{diff}} = 175$ days, $v_{\text{CSM}} = 100 \text{ km s}^{-1}$, and $\kappa = 0.34 \text{ cm}^2 \text{ g}^{-1}$, we get

$$\dot{M} \sim 0.9 M_{\odot} \text{ yr}^{-1}. \quad (14)$$

This is a very rough estimate but we can see that the mass-loss rate is high.

The fact that the LC can be fitted by the diffusion model indicates that the dense part of the CSM is swept-up at early times, and thus the dense part of the CSM is small in radius. As is discussed in M13, this is naturally expected for the $s > 3$ dense CSM. However, the diffusion model just requires the existence of the dense CSM near the progenitor. Thus, we cannot constrain the possibility that there exists a very dense $s < 3$ CSM with a small radius.

3.3 SN 2006aa

The bolometric LC of SN 2006aa could not be fitted by the M13 model as is the case for SN 2005kj. Again, the LC can be fitted by the diffusion model as shown in Fig. 2. We set the time of the peak luminosity as $t_p = 50$ days since the explosion and we get $\tau_{\text{diff}} = 163 \pm 25$ days, $\tau_{\text{exp}} = 22 \pm 5$ days, and $L_0 = (2.85 \pm 0.05) \times 10^{42} \text{ erg s}^{-1}$ with the statistical errors. By using Equation (13), the mass-loss rate can be roughly estimated as $\sim 0.8 M_{\odot} \text{ yr}^{-1}$.

3.4 SN 2006bo

The bolometric LC of SN 2006bo can be successfully fitted by the $L = L_1 t^\alpha$ formula (Fig. 3). The explosion date is set as 20 days before the discovery but it is not well-constrained (T13). The result is

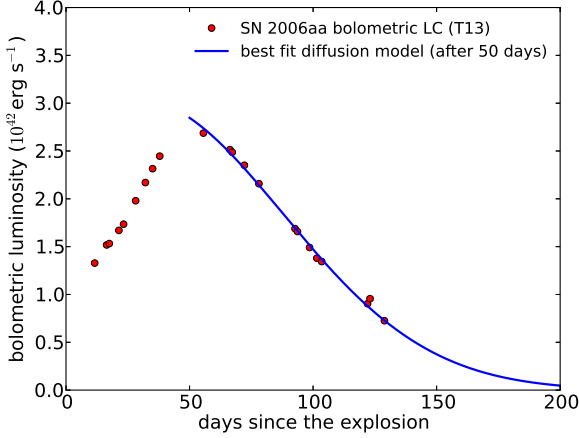


Figure 2. Bolometric LC of SN 2006aa (T13) and its fit to the diffusion model. The LC peak is assumed to be at 50 days since the explosion.

$$L = (1.03 \pm 0.06) \times 10^{43} \left(\frac{t}{1 \text{ day}} \right)^{-0.627 \pm 0.014} \text{ erg s}^{-1}. \quad (15)$$

The obtained $\alpha = -0.627 \pm 0.014$ corresponds to $s = 2.44 \pm 0.03$ ($n = 10$) or $s = 2.49 \pm 0.03$ ($n = 12$). The CSM density structure estimated for the $s = 2.44$ case is

$$\rho_{\text{csm}}(r) = 2.5 \times 10^{-15} \left(\frac{r}{10^{15} \text{ cm}} \right)^{-2.44} \text{ g cm}^{-3}. \quad (16)$$

The Thomson optical depth above 10^{15} cm (the shell radius is mostly above 10^{15} cm) for solar-metallicity CSM is 0.66 so our model is self-consistent. The mass-loss history estimated from the CSM density structure is

$$\dot{M}(t') = 9.1 \times 10^{-3} \left(\frac{v_{\text{csm}}}{100 \text{ km s}^{-1}} \right)^{0.56} \left(\frac{t'}{1 \text{ year}} \right)^{-0.44} M_{\odot} \text{ yr}^{-1}, \quad (17)$$

where t' is the time before the explosion. Note that we have ignored the bolometric luminosity data at around 170 days since the explosion when we fit the LC. The bolometric luminosity is significantly smaller than the previous epochs. As the bolometric LC is constructed by using near-infrared photometry as well, this sudden luminosity decline is not necessarily from the dust formation. We suspect that the shock has already gone out of the dense CSM at this epoch. This indicates that the high mass-loss rate of the progenitor does not last long enough for dense CSM to reach the corresponding radius (see Section 4.1).

3.5 SN 2006jd

The CSM properties estimated from the bolometric LC of SN 2006jd were presented in M13. The LC fitting with the $L = L_1 t^\alpha$ law results in

$$L = (3.9 \pm 0.1) \times 10^{42} \left(\frac{t}{1 \text{ day}} \right)^{-0.0708 \pm 0.0064} \text{ erg s}^{-1}, \quad (18)$$

with the statistical error. The power $\alpha = -0.0708 \pm 0.0064$ indicates $s = 1.40 \pm 0.01$ ($n = 10$) or $s = 1.62 \pm 0.01$ ($n = 12$). The CSM density structure for the $s = 1.40$ case is

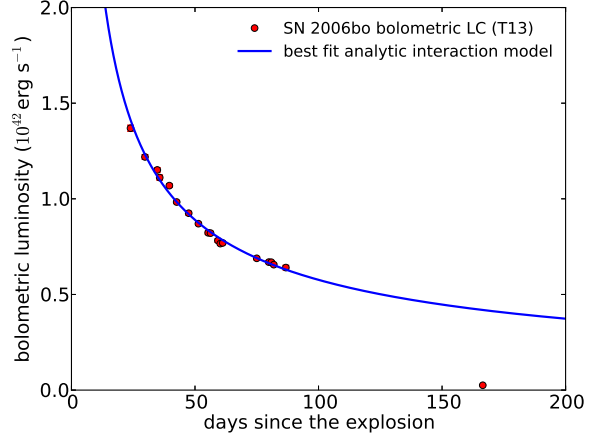


Figure 3. Bolometric LC of SN 2006bo obtained in T13 and its fit to the $L = L_1 t^\alpha$ formula.

$$\rho_{\text{csm}}(r) = 2.6 \times 10^{-16} \left(\frac{r}{10^{15} \text{ cm}} \right)^{-1.40} \text{ g cm}^{-3}. \quad (19)$$

The corresponding mass-loss rate is

$$\dot{M}(t') = 2.6 \times 10^{-4} \left(\frac{v_{\text{csm}}}{100 \text{ km s}^{-1}} \right)^{1.6} \left(\frac{t'}{1 \text{ year}} \right)^{0.6} M_{\odot} \text{ yr}^{-1}, \quad (20)$$

where t' is the time before the explosion. The mass-loss rate decreases as the progenitor gets closer to the time of explosion. The rate is higher than $10^{-3} M_{\odot} \text{ yr}^{-1}$ until about 9 years before the explosion.

3.6 SN 2006qq

The bolometric LC of SN 2006qq cannot be fitted by the $L = L_1 t^\alpha$ model because of the small t_t . Thus, we use the asymptotic formula to fit the LC. The asymptotic formula does not generally have an analytic form. We solve the equation numerically and see whether the fit is good or not by eyes. We assume that the explosion date is 16 days before the discovery (T13). We find that the $s = 2.0$ asymptotic model provides a good fit (Fig. 4). Thus, we conclude that the mass loss of the progenitor is fully consistent with being steady and we assign $s = 2.0$ for SN 2006qq in the following discussion. The spectral observations of T13 indicate that the shock velocity is almost constant with $10,000 \text{ km s}^{-1}$, which is consistent with the asymptotic model. Including the velocity evolution, the CSM density structure is estimated as

$$\rho_{\text{csm}}(r) = 1.1 \times 10^{-14} \left(\frac{r}{10^{15} \text{ cm}} \right)^{-2.0} \text{ g cm}^{-3}. \quad (21)$$

The CSM optical depth becomes unity at around 3×10^{15} cm. As $s = 2.0$, the mass-loss rate of the progenitor is constant

$$\dot{M}(t') = 2.1 \times 10^{-2} \left(\frac{v_{\text{csm}}}{100 \text{ km s}^{-1}} \right) M_{\odot} \text{ yr}^{-1}. \quad (22)$$

3.7 SN 2008fq

Since the bolometric LC of SN 2008fq cannot be fitted by the $L = L_1 t^\alpha$ formula self-consistently, we use the asymptotic

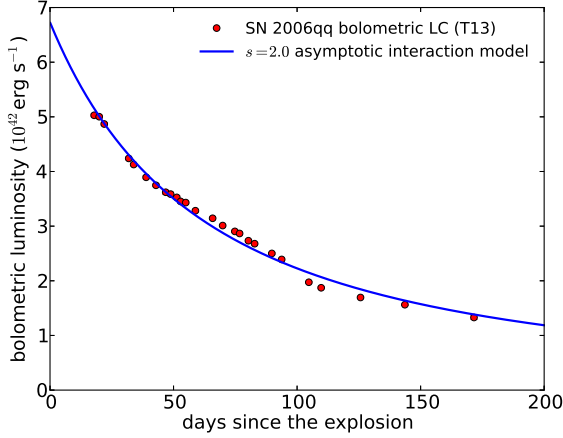


Figure 4. Bolometric LC of SN 2006qq (T13) and its fit to the $s = 2.0$ asymptotic LC model presented in M13. The $L = L_1 t^\alpha$ model fails because of a small t_t .

one. We assume that the explosion date is 8 days before the discovery (T13). If we assume $M_{\text{ej}} = 10 M_\odot$, the required CSM mass to fit the LC becomes very large (about $50 M_\odot$ within 10^{16} cm). Hence, we assume $M_{\text{ej}} = M_\odot$ instead for SN 2008fq. Then, we find that

$$\rho_{\text{CSM}}(r) = 3.8 \times 10^{-14} \left(\frac{r}{10^{15} \text{ cm}} \right)^{-2.1} \text{ g cm}^{-3}, \quad (23)$$

with $E_{\text{ej}} = 1.3 \times 10^{51}$ erg provides a better fit than the $s = 2.0$ or $s = 2.2$ models (Fig. 5). Thus, we assign $s = 2.1 \pm 0.05$ for SN 2008fq. The Thomson optical depth above 10^{15} cm is 12. The high optical depth is consistent with the existence of the early long rise time when the photons emitted from the shell are presumed to be scattered in the optically thick CSM. The corresponding mass-loss history is

$$\dot{M}(t') = 8.6 \times 10^{-2} \left(\frac{v_{\text{CSM}}}{100 \text{ km s}^{-1}} \right)^{0.9} \left(\frac{t'}{1 \text{ year}} \right)^{-0.1} M_\odot \text{ yr}^{-1}, \quad (24)$$

where t' is the time before the explosion.

3.8 SN 2010jl

The bolometric LC modeling of SN 2010jl is discussed in M13. The bolometric LC is constructed by Zhang et al. (2012) based on their optical photometric observations. The LC can be fitted by the $L = L_1 t^\alpha$ law but t_t becomes very small and the $L = L_1 t^\alpha$ model is not self-consistent. We have applied the asymptotic model and we obtain the CSM density structure

$$\rho_{\text{CSM}}(r) = 2.5 \times 10^{-14} \left(\frac{r}{10^{15} \text{ cm}} \right)^{-2.2} \text{ g cm}^{-3}, \quad (25)$$

assuming $M_{\text{ej}} = 10 M_\odot$ (M13). We again assign the statistical error of 0.05 and we use $s = 2.2 \pm 0.05$ for the SN 2010jl system in the next section. The mass-loss rate derived from Equation (25) is

$$\dot{M}(t') = 6.2 \times 10^{-2} \left(\frac{v_{\text{CSM}}}{100 \text{ km s}^{-1}} \right)^{0.8} \left(\frac{t'}{1 \text{ year}} \right)^{-0.2} M_\odot \text{ yr}^{-1}, \quad (26)$$

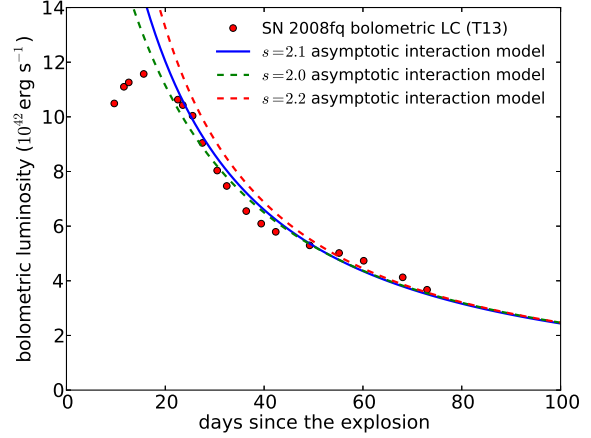


Figure 5. Bolometric LC of SN 2008fq from T13 and asymptotic LC models for the LC. The $L = L_1 t^\alpha$ model fails because of the small t_t . Based on the LC models in the figure with several s , we conclude that $s = 2.1$ provides the best fit to the LC after the peak.

where t' is the time before the explosion. The mass-loss rate recently reported by Fransson et al. (2013) is within a factor of a few ($0.11 M_\odot \text{ yr}^{-1}$). However, the mass-loss rate estimated by Ofek et al. (2013c) is about one order of magnitude higher and it is comparable to those of superluminous SNe (e.g., Moriya et al. 2013b). This may be because Ofek et al. (2013c) assume that the shock breakout occurred in the dense CSM while we do not. The shock breakout requires very high optical depth and thus, the large CSM mass.

3.9 SN 2011ht

The bolometric LC of SN 2011ht was constructed by Roming et al. (2012) based on their intensive near-ultraviolet and optical observations and we use their bolometric LC for our modeling (see also Pritchard et al. 2013). A pre-SN burst was detected in one year before the explosion of SN 2011ht (Fraser et al. 2013a). There is a suggestion that SN 2011ht may not be a true core-collapse event (Humphreys et al. 2012) but we assume it is. The bolometric LC is shown in Fig. 6. In the first two observational epochs, the bolometric luminosity declines. Thus, we assume that the first observed epoch is shortly after the explosion and we set the explosion date one day before the first observed epoch.

Fig. 6 shows the result of our bolometric LC fitting. The $L = L_1 t^\alpha$ law does not work self-consistently and we use the asymptotic form. As the asymptotic $s = 2.0$ model provides a good fit, we assign $s = 2.0$ for SN 2011ht. The CSM density structure is constrained to

$$\rho_{\text{CSM}}(r) = 5.0 \times 10^{-15} \left(\frac{r}{10^{15} \text{ cm}} \right)^{-2.0} \text{ g cm}^{-3}. \quad (27)$$

The Thomson optical depth becomes unity at 5×10^{15} cm. The corresponding mass-loss rate is

$$\dot{M}(t') = 1.0 \times 10^{-2} \left(\frac{v_{\text{CSM}}}{100 \text{ km s}^{-1}} \right) M_\odot \text{ yr}^{-1}. \quad (28)$$

The estimated mass-loss rate is consistent with

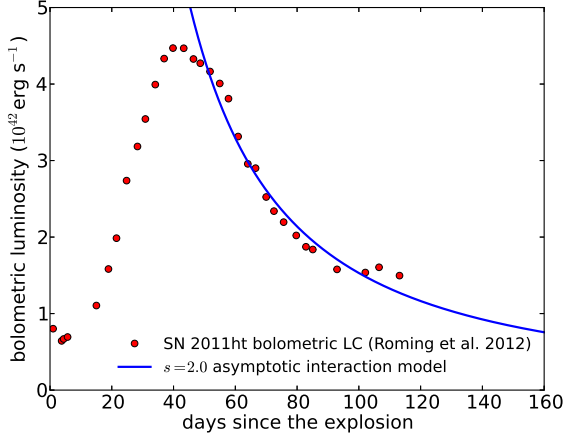


Figure 6. Bolometric LC of SN 2011ht (Roming et al. 2012) and the $s = 2.0$ asymptotic LC model for it.

those estimated in the previous studies, i.e., $0.03 M_{\odot} \text{ yr}^{-1}$ (Mauerhan et al. 2013a) and $0.05 M_{\odot} \text{ yr}^{-1}$ (Humphreys et al. 2012).

3.10 SN 1998S

The bolometric LC of SN 1998S is constructed by Fassia et al. (2000) based on their photometric observations in a wide spectral range. They obtain two bolometric LCs for SN 1998S depending on the way they fit the spectral energy distribution. We show their ‘spline’ bolometric LC instead of the ‘blackbody’ one. The choice of the bolometric LC does not affect our conclusion below.

We find that the bolometric LC of SN 1998S declines much faster than those we have modeled so far (Fig. 7). The LC in 100 days after the peak can be fitted by an exponential function

$$L = L_0 \exp\left(-\frac{t - t_p}{26 \pm 5 \text{ days}}\right). \quad (29)$$

This LC form is expected in the diffusion model when $\tau_{\text{diff}} = 26 \pm 5$ days and $t - t_p \ll 2\tau_{\text{exp}}$ (see Equation (10)). This indicates that the expansion timescale of SN 1998S is very large. This can be due to the efficient deceleration of the ejecta because of the SN-CSM collision. The fast declining LC may also be related to the asphericity of the dense CSM (Section 4.3).

We can roughly estimate the mass-loss rate of the progenitor with τ_{diff} by Equation (13). Assuming $v_{\text{CSM}} = 100 \text{ km s}^{-1}$ and $\kappa = 0.34 \text{ cm}^2 \text{ g}^{-1}$, we obtain the rough mass-loss rate of $\dot{M} \sim 0.01 M_{\odot} \text{ yr}^{-1}$. The estimated mass-loss rate is rather high compared with those estimated by the previous studies ($10^{-4} - 10^{-3} M_{\odot} \text{ yr}^{-1}$, see Kiewe et al. 2012 for a summary).

3.11 SN 2009ip

The major luminosity increase of SN 2009ip in 2012 was observed intensively by many groups. There is discussion about whether it is really a core-collapse event or not

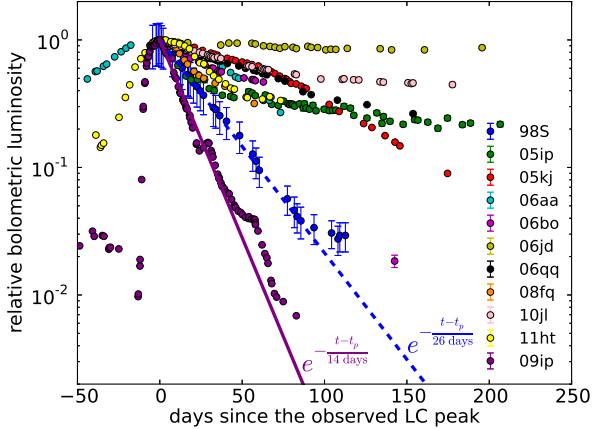


Figure 7. Bolometric LCs of SN 1998S and SN 2009ip in 2012 compared with the other SN IIn LCs in this paper. The two LCs can be fitted by a single exponential function as indicated in the figure.

(e.g., Smith, Mauerhan, & Prieto 2013; Fraser et al. 2013a; Pastorello et al. 2013; Martin et al. 2013) but here we assume that the final brightening is due to a SN explosion. We use the bolometric LC reported by Fraser et al. (2013a) for our modeling (see also Margutti et al. 2014). As was the case for SN 1998S, the LC declines fast and it can be fitted by an exponential function (Fig. 7). The diffusion timescale τ_{diff} is 14 ± 1 days. The corresponding mass-loss rate for the standard set of the parameters is $\dot{M} \sim 9 \times 10^{-3} M_{\odot} \text{ yr}^{-1}$. This mass-loss rate is consistent with those estimated by Fraser et al. (2013a) ($10^{-2} - 10^{-1} M_{\odot} \text{ yr}^{-1}$) and Ofek et al. (2013a) ($10^{-3} - 10^{-2} M_{\odot} \text{ yr}^{-1}$). Baklanov et al. (2013) presents a LC model of SN 2009ip to demonstrate the dense shell method which is a newly-proposed method to use SNe IIn as a primary standard candle (cf. Potashov et al. 2013). The CSM density slope is $s = 3$ and the average mass-loss rate is $10^{-2} M_{\odot} \text{ yr}^{-1}$ with $v_{\text{CSM}} = 100 \text{ km s}^{-1}$, which is consistent with our result.

4 DISCUSSION

We summarize the CSM properties and corresponding mass-loss histories of SN IIn progenitors estimated in the previous section here. We have applied our bolometric LC model to the observed ones until around 100-200 days since the explosion. The CSM shocked at these epochs are released from the progenitors within about 30-60 years before their explosions and, the following mass-loss histories we discuss correspond to those decades before the explosions. This is because the typical CSM velocity of SN IIn progenitors which is observed in very narrow P Cygni components of SNe IIn is $\sim 100 \text{ km s}^{-1}$ (e.g., T13; Kiewe et al. 2012), while the typical shocked shell velocity is $\sim 10,000 \text{ km s}^{-1}$. As the SN shock propagates about 100 times faster, it should have taken 100 times longer for the CSM to reach the same radius.

4.1 Overall mass-loss properties

Fig. 8 summarizes the estimated CSM density slope s ($\rho_{\text{CSM}} \propto r^{-s}$). When we can fit the bolometric LCs by the $L = L_1 t^\alpha$ law self-consistently, we can estimate s only from the bolometric LCs by assuming n . In Fig. 8, we plot two s , one expected from $n = 10$ (circle) and another from $n = 12$ (square). When we apply the asymptotic model, we only plot one s for each SN. There are four cases for which we apply the diffusion model. This may arise from $s > 3$ CSM and we indicate these by arrows.

Looking at Fig. 8, we can find that many s gather around 2. This means that the mass loss of these SN IIn progenitors within decades before the explosions is constantly large. In other words, many SN IIn progenitors are likely to keep their high mass-loss rates within the decades before their explosion. In addition, there may exist a preference for s to be larger than 2. Assuming that the CSM velocity does not change much during the last stage of the stellar evolution, the preference to $s > 2$ means that the mass-loss rates of SN IIn progenitors increase as the progenitors get closer to the time of the explosion. Note, however, that the systematic error is uncertain and can be important. For instance, the uncertainty in the estimated explosion dates is sometimes large. Nonetheless, the deviation from the steady mass loss in SN IIn CSM has been suggested in previous studies as well. For example, Dwarkadas & Gruszko (2012) collected SN X-ray LCs and found that SN IIn X-ray LCs are mostly not consistent with the $s = 2$ CSM.

Fig. 9 presents the history of the mass-loss rates of SN IIn progenitors estimated in the previous section. We need to assume the SN ejecta properties in some cases and the uncertainty of the history is expected to be large. The longest time we can trace depends on the time we used to fit the bolometric LCs. For SNe IIn for which we apply the diffusion model, we indicate the rough mass-loss rates estimated from the diffusion timescale (Equation (13)). The longest time traced in these cases is set by assuming that the entire dense CSM is swept up at the LC peak. The mass-loss rates we obtain are consistent with those obtained from other methods like $H\alpha$ luminosities which also indicate that the mass-loss rates are typically higher than $\sim 10^{-3} M_\odot \text{ yr}^{-1}$ (e.g., T13; Kiewe et al. 2012).

4.2 Mass-loss mechanisms of SN IIn progenitors

We have shown that the density slopes of dense CSM making SNe IIn are often close to $s = 2$. This indicates that the mass-loss rates of SN IIn progenitors are constantly high within decades before their explosion. In some SNe IIn, sudden luminosity increases of their progenitors a few years to ~ 10 days before their explosions have been observed and are related to the formation of the dense CSM (e.g., Pastorello et al. 2007; Prieto et al. 2013; Fraser et al. 2013b; Ofek et al. 2013b). SNe IIn for which we apply the diffusion model are mostly consistent with this timescale (Fig. 9) and these SN IIn progenitors may make the dense CSM by the eruptive mass loss. However, the progenitors of most SNe IIn we have modeled are found to have high mass-loss rates for decades. Thus, our results indicate that there exists some mechanism for the progenitors to sustain their high mass-loss rates at least for decades before their explosions. The

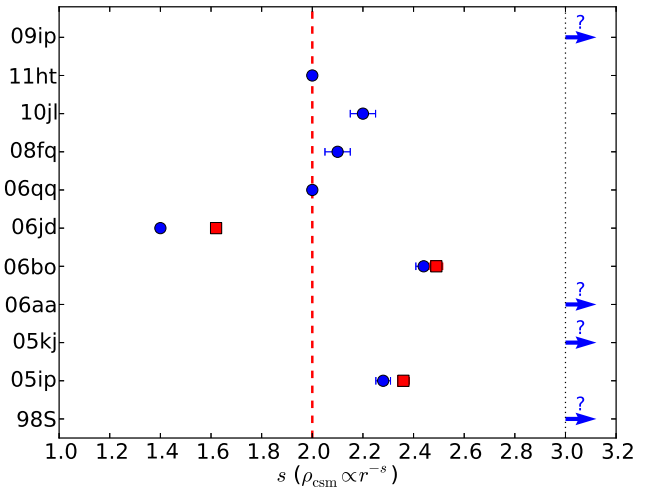


Figure 8. Estimated CSM density slopes s of the SN IIn progenitors. When we need to assume n to estimate s , we show the results of the cases of $n = 10$ (blue circle) and $n = 12$ (red square).

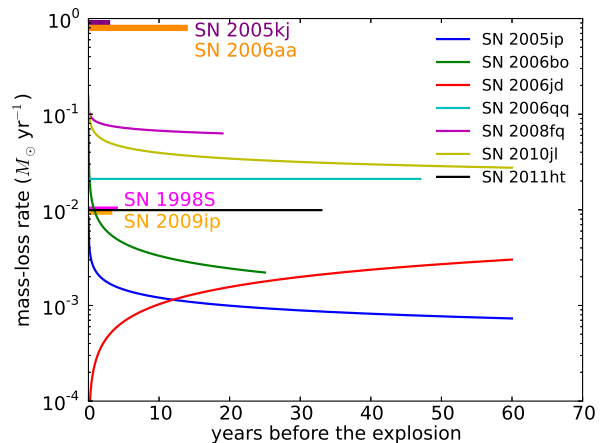


Figure 9. Estimated mass-loss histories of the SN IIn progenitors. The results of the $n = 10$ models are shown when we need to assume n . The shaded SNe (SNe 2005kj, 2006aa, 1998S, and 2009ip) are those for which we roughly estimate the mass-loss rates based on the diffusion model. $v_{\text{CSM}} = 100 \text{ km s}^{-1}$ is assumed in this figure.

observed eruptive events on shorter timescales do not explain all the dense CSM of SNe IIn. Those eruptive events may make the dense CSM which are not smooth. The existence of non-smooth dense CSM is indicated in some SN IIn LCs which show short-time variability (e.g., SN 2009ip, Margutti et al. 2014).

We have also found that the mass-loss rates of SN IIn progenitors may preferentially get higher as they get closer to the time of the explosion. However, mass loss which occurs at the surface of a star and the core collapse which occurs at the center of the star are usually not physically connected to each other. If the mass-loss rates of SN IIn progenitors truly tend to increase towards their time of the core collapse, this may indicate that the high mass-loss rates of SN IIn progenitors are somehow related to the core evolution of the

progenitors. There are several mechanisms to enhance the mass-loss rates which are triggered by the core evolution towards the core collapse and our result may support such mechanisms.

For example, Quataert & Shiode (2012); Shiode & Quataert (2014) suggest that the g-mode wave which is excited by the convective motion at the core can convey energy to the surface. The conveyed energy can trigger the mass loss at the surface. Since the convective motion can be more active as the nuclear burning proceeds, this mechanism may be able to explain the increasing mass-loss rates. Although Shiode & Quataert (2014) found that this mechanism may only work within about 10 years before the core collapse, it still remains a possible mechanism to enhance the mass loss towards the death. Another example is the violent convective motion caused by the unstable nuclear burning (e.g., Smith & Arnett 2013). This mechanism may also be enhanced as the nuclear burning advances since the advanced nuclear burning is more sensitive to temperature.

So far, we have emphasized the fact that the mass-loss rates of SN IIn progenitors may tend to increase as they get closer to the time of the explosion. However, there also exists an exception (SN 2006jd, see also Chandra et al. 2012a). In addition, the number of SNe IIn we show here is small and we are still not at a stage of making a strong statement from them. More SN IIn observations from which we can estimate bolometric LCs and apply our LC model are required to get a clearer view of the SN IIn mass loss.

4.3 Effect of asphericity

The bolometric LC model we applied to estimate the mass-loss rates so far assumes the spherical symmetry. However, the deviation from the spherical symmetry is reported in many SNe IIn (e.g., Patat et al. 2011; Trundle et al. 2009; Leonard et al. 2000; Levesque et al. 2014). In this section, we briefly discuss the effect of the asphericity on the bolometric LCs and the mass-loss rates estimated in this paper.

The significant effect of the CSM asphericity on the bolometric LCs is in the reduction of the dense CSM decelerating the SN ejecta. The dense part of the CSM exists in all the directions in the spherically symmetric case while the dense part only exists in some directions in the aspherical case. If the Thomson optical depth of the dense CSM is less than unity, as is the case for the most SNe IIn we model here, the photons emitted from the shock will be directly observed. Thus, the bolometric luminosity is presumed to be roughly proportional to the degree of the asymmetry for a given CSM density. In other words, the bolometric luminosity is expected to be reduced by the amount of the dense CSM decreased by the asymmetry for a given CSM density. If the dense CSM with $\rho_{\text{CSM}} = Dr^{-s}$ exists only at the Ω direction out of 4π , the average CSM density decreases to $\langle\rho_{\text{CSM}}\rangle = \frac{\Omega}{4\pi}Dr^{-s}$. Here, we assume that the density of the sparse part of the CSM is significantly smaller than that of the dense part. The effect of the decrease in the average CSM density caused by the asphericity on the luminosity is roughly included in the efficiency ϵ in our model. The efficiency will be decreased by $\frac{\Omega}{4\pi}$ by the asymmetry because of the reduction of the average CSM density. This means that the mass-loss rate of the Ω direction should be

increased by $\frac{4\pi}{\Omega}$ to get the same luminosity as the spherically symmetric case so that the dense part of the CSM will be $\rho_{\text{CSM}} = \frac{4\pi}{\Omega}Dr^{-s}$. However, even though the mass-loss rate should be increased in the Ω direction to get the same luminosity, the average mass-loss rate remains the same as the mass-loss rate obtained by the spherically symmetric model because the average density of the entire CSM becomes $\langle\rho_{\text{CSM}}\rangle = Dr^{-s}$. Thus, although the mass-loss rate of a particular direction should be increased, the average mass-loss rate is expected to remain roughly the same as the spherically symmetric case to have the same luminosity in the aspherical case.

If the dense part of the CSM is optically thick, the effect of the diffusion in the aspherical CSM is presumed to be significant and the aspherical CSM can change the LCs more significantly, depending on the viewing angle of the observers. Some bolometric LCs shown in this paper are found to decline much faster than those expected from the analytic model (SNe 2005kj, 2006aa, 1998S, and 2009ip). In the case of the optically thin CSM, the deviation from the spherical symmetry is presumed to change the efficiency mainly without changing the LC shape significantly. In addition, an interesting common property of the fast-declining LCs is that their luminosities decline exponentially. The exponential decay is not naturally expected from the asphericity of the optically-thin CSM. As we discussed earlier, the exponential decay is naturally expected from the diffusion in the shocked optically-thick dense CSM. Interestingly, the bolometric LCs of SNe 1998S and 2009ip, whose LC declines are much faster than other SNe IIn, are suggested to have a large asymmetry (Fassia et al. 2000; Leonard et al. 2000; Levesque et al. 2014). Since the diffusion process is significantly affected by the asymmetry, these fast declines may be related to the asphericity and the viewing angle of the observers.

We have discussed the possible effect of the deviation from the spherical symmetry assumed in the analytic LC model qualitatively in this section. However, the aspherical effect should be eventually investigated quantitatively. We leave this as our future work.

5 CONCLUSION

We have presented the results of our systematic study of the CSM around SNe IIn. To estimate the CSM properties, we apply an analytic bolometric LC model for interacting SNe formulated in M13 to 11 SN IIn bolometric LCs. We have reconstructed the mass-loss histories of SN IIn progenitors based on the estimated CSM properties. As we typically use the bolometric LCs within 200 days since the explosion, we are able to trace the mass-loss histories within about 60 years before the explosion.

We find that mass-loss rates of many SNe IIn are constantly high (above $\sim 10^{-3} M_{\odot} \text{ yr}^{-1}$) for more than a decade before their explosion (Fig. 9). This suggests that the eruptive mass loss with shorter timescales observed in several SN IIn progenitors is not always a mechanism to make the dense CSM. There should be a mass-loss mechanism which sustains the high mass-loss rates at least for decades before the explosion. In addition, we find that SN IIn progenitors may tend to increase their mass-loss rates

as they get closer to the time of the explosion. If this is confirmed, the currently unknown mass-loss mechanism of SN IIn progenitors may be related to the core evolution of them. However, the number of SNe IIn we modeled is still small and we need more SN IIn observations from which we can construct bolometric LCs.

Revealing the progenitors of SNe IIn is important for the understanding of not only SNe but also stellar evolution. SN IIn progenitors provide us with a clue to find missing keys in the current stellar evolution theory. Some progenitor and mass-loss properties are starting to be revealed as we show here in this paper. However, we need more efforts to reach a better understanding of them.

ACKNOWLEDGEMENTS

We would like to thank the referee for the comments which improved this paper. T.J.M. is supported by the Japan Society for the Promotion of Science Research Fellowship for Young Scientists (23-5929). K.M. acknowledges the financial support by a Grant-in-Aid for Scientific Research for Young Scientists (23740141). This research is also supported by World Premier International Research Center Initiative (WPI Initiative), MEXT, Japan. The Oskar Klein Centre is funded by the Swedish Research Council. The work in Russia was supported by RF Government grant 11.G34.31.0047, grants for supporting Scientific Schools 5440.2012.2 and 3205.2012.2, and joint RFBR-JSPS grant 13-02-92119.

REFERENCES

- Anderson J. P., Haberman S. M., James P. A., Hamuy M., 2012, *MNRAS*, 424, 1372
- Arnett W. D., 1980, *ApJ*, 237, 541
- Baklanov P. V., Blinnikov S. I., Potashov M. Sh., Dolgov A. D., 2013, *JTEP Letters*, 98, 432
- Blinnikov S. I., Bartunov O. S., 1993, *A&A*, 273, 106
- Blinnikov S. I., Eastman R., Bartunov O. S., Popolitov V. A., Woosley S. E., 1998, *ApJ*, 496, 454
- Blinnikov S. I., Röpke F. K., Sorokina E. I., Gieseler M., Reinecke M., Travaglio C., Hillebrandt W., Stritzinger M., 2006, *A&A*, 453, 229
- Chandra P., Chevalier R. A., Chugai N., Fransson C., Irwin C. M., Soderberg A. M., Chakraborti S., Immler S., 2012a, *ApJ*, 755, 110
- Chandra P., Chevalier R. A., Irwin C. M., Chugai N., Fransson C., Soderberg A. M., 2012b, *ApJ*, 750, L2
- Chevalier R. A., Fransson C., 2006, *ApJ*, 651, 381
- Chevalier R. A., Fransson C., Nymark T. K., 2006, *ApJ*, 641, 1029
- Chugai N. N., Danziger I. J., 1994, *MNRAS*, 268, 173
- Dwarkadas V. V., Gruszko J., 2012, *MNRAS*, 419, 1515
- Fassia A., et al., 2000, *MNRAS*, 318, 1093
- Fox O. D., Filippenko A. V., Skrutskie M. F., Silverman J. M., Ganeshalingam M., Cenko S. B., Clubb K. I., 2013, *AJ*, 146, 2
- Fox O. D., et al., 2011, *ApJ*, 741, 7
- Fransson C., et al., 2013, *arXiv*, arXiv:1312.6617
- Fransson C., et al., 2002, *ApJ*, 572, 350
- Fraser M., et al., 2013a, *MNRAS*, 433, 1312
- Fraser M., et al., 2013b, *ApJ*, 779, L8
- Gal-Yam A., Leonard D. C., 2009, *Natur*, 458, 865
- Groh J. H., Meynet G., Ekström S., 2013, *A&A*, 550, L7
- Humphreys R. M., Davidson K., 1994, *PASP*, 106, 1025
- Humphreys R. M., Davidson K., Jones T. J., Pogge R. W., Grammer S. H., Prieto J. L., Pritchard T. A., 2012, *ApJ*, 760, 93
- Katsuda S., Maeda K., Nozawa T., Pooley D., Immler S., 2014, *ApJ*, 780, 184
- Kiewe M., et al., 2012, *ApJ*, 744, 10
- Langer N., 2012, *ARA&A*, 50, 107
- Leonard D. C., Filippenko A. V., Barth A. J., Matheson T., 2000, *ApJ*, 536, 239
- Levesque E. M., Stringfellow G. S., Ginsburg A. G., Bally J., Keeney B. A., 2014, *AJ*, 147, 23
- Maeda K., et al., 2013, *ApJ*, 776, 5
- Margutti R., et al., 2014, *ApJ*, 780, 21
- Martin J. C., Hamsch F.-J., Margutti R., Tan T.-G., Curtis I., Soderberg A., 2013, *arXiv*, arXiv:1308.3682
- Matzner C. D., McKee C. F., 1999, *ApJ*, 510, 379
- Mauerhan J. C., et al., 2013a, *MNRAS*, 431, 2599
- Mauerhan J. C., et al., 2013b, *MNRAS*, 430, 1801
- Moriya T. J., Blinnikov S. I., Baklanov P. V., Sorokina E. I., Dolgov A. D., 2013a, *MNRAS*, 430, 1402
- Moriya T. J., Blinnikov S. I., Tominaga N., Yoshida N., Tanaka M., Maeda K., Nomoto K., 2013b, *MNRAS*, 428, 1020
- Moriya T. J., Maeda K., Taddia F., Sollerman J., Blinnikov S. I., Sorokina E. I., 2013c, *MNRAS*, 2032 (M13)
- Ofek E. O., Lin L., Kouveliotou C., Younes G., Göğüş E., Kasliwal M. M., Cao Y., 2013a, *ApJ*, 768, 47
- Ofek E. O., et al., 2013b, *Natur*, 494, 65
- Ofek E. O., et al., 2013c, *arXiv*, arXiv:1307.2247
- Pastorello A., et al., 2007, *Natur*, 447, 829
- Pastorello A., et al., 2013, *ApJ*, 767, 1
- Patat F., Taubenberger S., Benetti S., Pastorello A., Harutyunyan A., 2011, *A&A*, 527, L6
- Potashov M., Blinnikov S., Baklanov P., Dolgov A., 2013, *MNRAS*, 431, L98
- Prieto J. L., Brimacombe J., Drake A. J., Howerton S., 2013, *ApJ*, 763, L27
- Prieto J. L., et al., 2008, *ApJ*, 681, L9
- Pritchard T. A., Roming P. W. A., Brown P. J., Bayless A. J., Frey L. H., 2013, *arXiv*, arXiv:1303.1190
- Quataert E., Shiode J., 2012, *MNRAS*, 423, L92
- Roming P. W. A., et al., 2012, *ApJ*, 751, 92
- Schlegel E. M., 1990, *MNRAS*, 244, 269
- Shiode J. H., Quataert E., 2014, *ApJ*, 780, 96
- Smith N., Arnett D., 2013, *arXiv*, arXiv:1307.5035
- Smith N., Mauerhan J., Prieto J., 2013, *arXiv*, arXiv:1308.0112
- Smith N., McCray R., 2007, *ApJ*, 671, L17
- Smith N., Li W., Silverman J. M., Ganeshalingam M., Filippenko A. V., 2011, *MNRAS*, 415, 773
- Stritzinger M., et al., 2012, *ApJ*, 756, 173
- Taddia F., et al., 2013, *A&A*, 555, A10 (T13)
- Trundle C., et al., 2009, *A&A*, 504, 945
- Zhang T., et al., 2012, *AJ*, 144, 131

APPENDIX A: COMPARISON WITH NUMERICAL CALCULATION

In M13, some results of numerical LC calculations based on the initial conditions obtained by the analytic model are presented. Here, we show more detailed comparison between the analytic and numerical models. We focus on the SN 2005ip model. The parameters of the SN 2005ip progenitor system estimated from the analytic model by assuming $\delta = 1$, $n = 10$, $M_{\text{ej}} = 10 M_{\odot}$, and $\epsilon = 0.1$ are $E_{\text{ej}} = 1.2 \times 10^{52}$ erg and $\rho_{\text{csm}}(r) = 8.4 \times 10^{-16} (r/10^{15} \text{ cm})^{-2.28} \text{ g cm}^{-3}$. We set the outer radius of the CSM at 5×10^{16} cm. The numerical radiation hydrodynamics calculation is performed by STELLA, which is a one-dimensional radiation hydrodynamics code (e.g., Blinnikov et al. 2006; Blinnikov & Bartunov 1993). In STELLA, the conversion efficiency from kinetic energy to radiation, which corresponds to ϵ in the analytic model, is controlled by the smearing parameter (Blinnikov et al. 1998; Moriya et al. 2013b). We set the smearing parameter so that ϵ gets close to 0.1, which is assumed in the analytic model.

Fig. A1 shows the LCs obtained from the numerical calculation and the analytic model. Overall, the two LCs match, although the numerical LC is brighter until about 25 days since the explosion. Figs A2 and A3 compare the radii and velocities of the numerical results to the analytic estimates. Both the radius and velocity obtained from the numerical result are a bit higher than the analytic expectations. However, the difference is within 10 %.

We finally estimate the conversion efficiency ϵ from the numerical calculation. The conversion efficiency is defined as

$$\epsilon = L \left(\frac{dE_{\text{kin}}}{dt} \right)^{-1}. \quad (\text{A1})$$

L is directly obtained by the numerical result. To estimate dE_{kin}/dt from the numerical simulation, we assume that the shell velocity v_{sh} does not change much during a very small time Δt . Then, by using the CSM mass ΔM swept up during Δt , the total available kinetic energy ΔE_{kin} during Δt can be approximated as

$$\Delta E_{\text{kin}} = \frac{1}{2} \Delta M v_{\text{sh}}^2, \quad (\text{A2})$$

$$\simeq 2\pi D r_{\text{sh}}^{2-s} v_{\text{sh}}^3 \Delta t. \quad (\text{A3})$$

Then, ϵ can be approximated as

$$\epsilon \simeq L \left(\frac{\Delta E_{\text{kin}}}{\Delta t} \right)^{-1} = \frac{L}{2\pi D r_{\text{sh}}^{2-s} v_{\text{sh}}^3}, \quad (\text{A4})$$

and we can estimate ϵ from L , r_{sh} , and v_{sh} , which are available from the numerical calculation.

Fig. A4 shows the efficiency obtained from the numerical calculation. At early times, the efficiency gets large for a short period of time but it becomes almost constant at around 0.1 later. The assumption of the constant efficiency may not be valid in the early times but it is a good approximation in most of time. This means that the LC shape is mainly determined by the change in the density, not by the change in the efficiency.

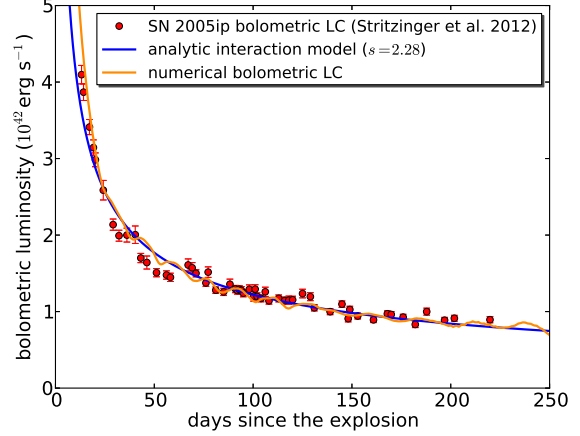


Figure A1. Observed, analytic, and numerical LCs of SN 2005ip.

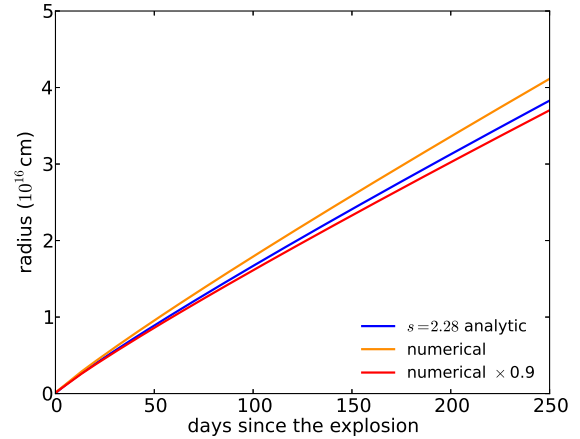


Figure A2. Radial evolution obtained from the analytic model and that from numerical calculation. We also show a line which is 90% of the numerical result.

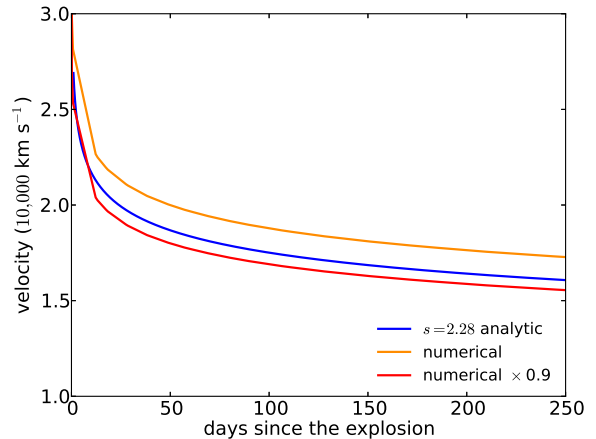


Figure A3. The same as Fig. A2 but for the velocity.

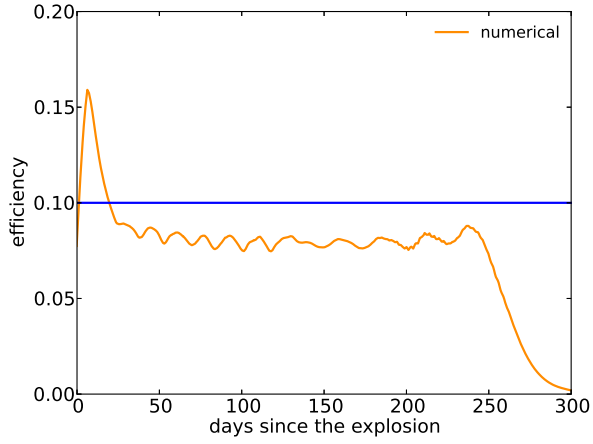


Figure A4. Efficiency of the conversion from the available kinetic energy to radiation in the numerical model. The efficiency is estimated from Equation (A4).